SCIENCE CHINA
Information Sciences

• RESEARCH PAPER •

August 2016, Vol. 59 082305:1–082305:13
doi: 10.1007/s11432-016-5556-2

Hybrid inter-cell interference management for ultra-dense heterogeneous network in 5G

Chen HUANG, Qianbin CHEN* & Lun TANG

Key Laboratory of Mobile Communication Technology, School of Communication and Information Engineering, Chongqing University of Posts and Telecommunications, Chongqing 400065, China

Received November 5, 2015; accepted January 21, 2016; published online April 25, 2016

Abstract The Ultra-dense Heterogeneous Network (HetNet), which consists of macro-cells and pico-cells, has been recognized as a key technique to improve network performance. However, the increasing number of pico-cells also causes severe interference including inter-cell interference and intra-cell interference. Therefore, interference management has become an important issue in ultra-dense HetNets, and the traditional enhanced inter-cell interference coordination (eICIC) scheme is no longer fit for the high density of small cells. In this paper, a hybrid interference management method based on dynamic eICIC and coordinated multi-point transmission (CoMP) is proposed. Firstly, a virtual cell is established based on the characteristics of ultra dense HetNets. Then, a novel joint dynamic eICIC scheme combined with multi-user beamforming is deployed to eliminate the inter-cell interference, and improve the throughput of virtual cell significantly without sharp decrease of throughput of macro-cell. Furthermore, a virtual cell based joint transmission scheme is deployed with a power control algorithm, which can obviously increase the spectrum efficiency of virtual cell edge. Simulation results verify that the proposed scheme can achieve better spectrum efficiency both at macro-cell and virtual cell edges, and the network throughput is also improved.

Keywords interference management, coordinated multi-point transmission, ultra dense network, almost blank subframe, spectrum efficiency

Citation Huang C, Chen Q B, Tang L. Hybrid inter-cell interference management for ultra-dense heterogeneous network in 5G. Sci China Inf Sci, 2016, 59(8): 082305, doi: 10.1007/s11432-016-5556-2

1 Introduction

In recent years, it has been witnessed that the data traffic over cellular networks grows up explosively, and the System spectral efficiency has been greatly improved with the development of technologies, such as the Heterogeneous-Network (HetNet), which consists of macro-cells and small-cells (femto-cell or pico-cell). Recently, much attention has been drawn to the Ultra-dense network (UDN), where a huge number of pico-cells are deployed close to mobile stations, so as to boost the network capacity. Four general directions can be taken to enhance the system throughput of HetNets: spectrum extension, better spectrum efficiency, higher network node density with pico-cells, and offloading. To improve the spectrum efficiency, frequency reuse factor tends to be set, which means macro-cells and pico-cells always share the same frequency.

* Corresponding author (email: chenqb@cqupt.edu.cn)

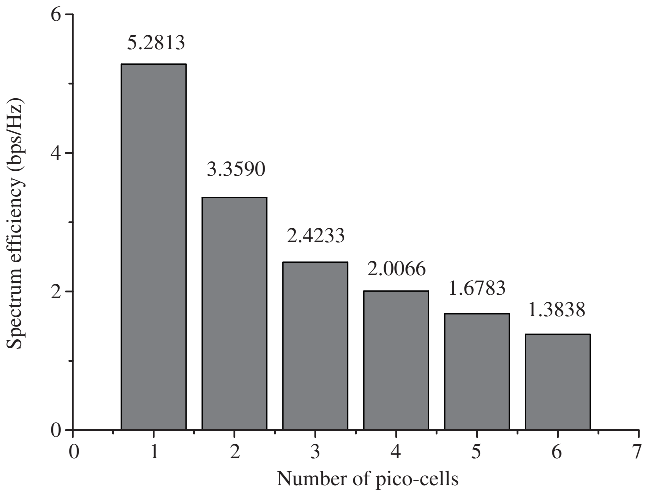

Figure 1 Spectrum efficiency comparison

However, since the density of the pico-cell increases to a crowding level, pico-cells are deployed much closer to each other, even to the macro e-node B (eNB). As a result, the inter-cell interference and the intra-cell interference from neighboring cells become a serious problem. The cell-edge users equipment (UE) in pico-cells always suffers considerable performance degradation due to the weak received signal power from their associated low power base stations. Accordingly, enhanced inter-cell interference coordination (eICIC) [1, 2] has been introduced as a key technology for interference management in LTE-A networks. By using the almost blank Subframes (ABS), eICIC technology can provide a good way for macro BSs and low power BSs to time-share the radio resources. The macro BS remains silent in ABS to eliminate the inter-cell interference, and the pico-cell can transmit in a low interference environment. However, the inter-cell interference in Ultra-dense HetNets is not the only reason causing the decrease of network performance. The high density of pico-cells leads to significant intra-cell interference, decreasing the throughput of cell-edge UEs.

To solve these problems, in the past, some eICIC schemes such as dynamic ABRB control [3] were proposed in LTE-A. And some other researches [4, 5] proposed the SCGM scheme, in which pico-cells in network always do not share the same ABS, in other words, different pico-cells have different ABS models to avoid the intra-cell interference between them. In these situations, different pico-cells can transmit in different ABSs, therefore, the throughput of pico-cells can be improved. However, the cost of these schemes is poor user experience of MUEs, because more pico-cells require more ABSs, while more ABSs mean more silent subframes for MUEs. As the number of pico-cells increases, the number of ABS model for different pico-cells in the same macro-cell is also increased. As a result, MUEs will have fewer and fewer subframes to transmit data, and the spectrum efficiency will decline significantly. If different pico-cells work in different frequencies, the increasing number of pico-cells might cause less spectrum resource for each pico-cell, which also leads to the falling of spectrum efficiency. Figure 1 shows how spectrum efficiency of one macro-cell(with three sector modes, including the pico-cells in its coverage) decreases with the number of pico-cells while different ABS models are used for different pico-cells.

As shown in Figure 1, the spectrum efficiency drops sharply with the increase of pico-cells. Usually the increase of pico-cells improves the spectrum efficiency and capacity in HetNets, but the huge number of pico-cells intricates channel environment and cell-edge UEs might suffer interference from neighbor eNB. Severe channel environment caused by interference has adverse impact on network performance in ultra-dense HetNets.

On the other hand, to efficiently improve the signal to interference plus noise ratio (SINR) of cell-edge UEs, the coordinated multi-point transmission (CoMP) technology has been applied in ultra-dense Network. The deployment and scenarios of this technology are defined in 3GPP Rel. 11 CoMP. As introduced in [6], downlink CoMP can be classified into joint transmission (JT), coordinated scheduling

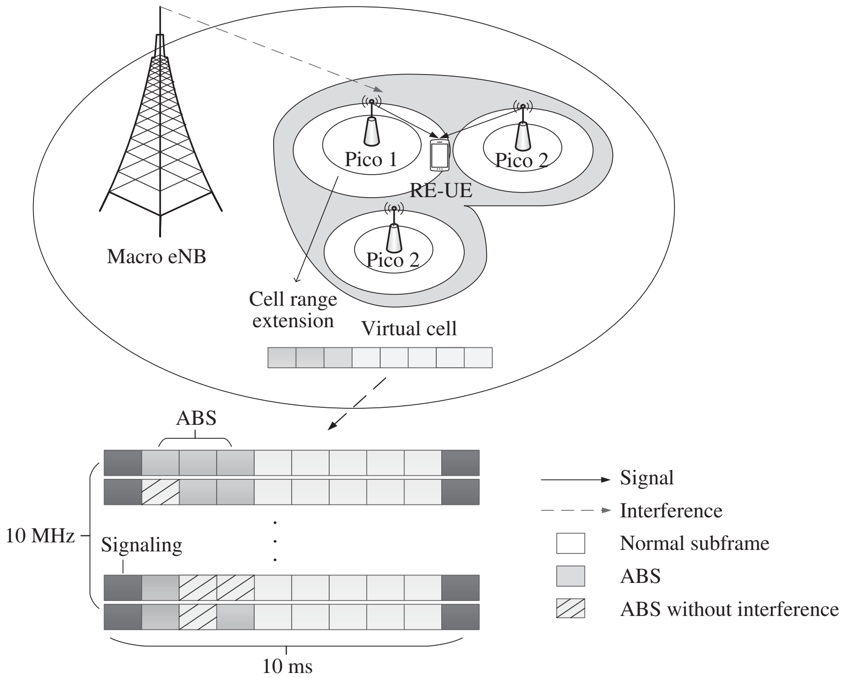

Figure 2 System model.

and coordinate beamforming (CS/CB) [7].

Recently, there are some research on interference management based on eICIC and CoMP, such as [8,9]. CoMP and eICIC schemes are overviewed, which can improve the cell edge throughput, but the study only focuses on the simple apply of the technology without getting into the details of factor-optimization. In [10], an optimization of time-domain resource allocation for ABS scheme is proposed. CoMP is implemented between macro-eNB and pico-eNB. Nevertheless, with the increase of pico-eNB number, joint transmission between pico-eNBs becomes more and more important with great research value.

In this paper, we consider *virtual cell* [11] for pico-cell management and *hybrid interference management* which combines the characteristics of eICIC and CoMP technology to control interference. We only consider the download link situation. In order to avoid the decrease of spectrum efficiency, all the pico-cells share the same ABS model in our project. In our scheme, the virtual cell is configured which consists of particular pico-cells close to each other, and the intra-cell interference can be utilized by joint transmission, as shown in Figure 2. The principle of how to choose the member of virtual cell is discussed in Section 4.

Simulation results show that the proposed scheme can significantly outperform the existing algorithms, and achieve the best performance both in pico-cells and in overall network.

The rest of this paper is organized as follows: In Section 2, we present the system model under the consideration of ultra-dense HetNets. In Section 3, we propose a scheme for inter cell interference management in ultra-dense network. In Section 4, we provide the details of our scheme improving spectrum efficiency even more.

2 System model

The system model is shown in Figure 2. We consider one M-eNB with M macro-cell MUEs and L pico-cell eNBs (P-eNBs) with cellular (L_0 L_N), and all eNBs share the same frequency spectrum to improve the spectrum efficiency. To simplify the analysis of the problem without loss of generality, we only consider one sector in the macro-cell and the overall network can triple the situation results simply. And we also assume there are N PUEs randomly distributed in the pico-cell. And in the rest of this paper, we only consider the downlink transmission.

Table 1 Notation definition

Notation	Definition
M	Number of MUE
L	Number of P-eNBs
N	Number of PUE in each picocell
α_i	Fraction of ABS in macro-cell
P_{M}, P_{P}	Transmission power of MUE and PUE
P_{Max}	Maximum of transmission power
B	System bandwidth
δ^2	Noise power per PRB bandwidth in the licensed band
R_{M}, R_{V}	Throughput of macro cells and virtual cells
R_{Min}, R_{T}	Minimum of throughput and Threshold of throughput
$\mathrm{RSRP}^{\mathrm{a}}$, $\mathrm{RSRP}^{\mathrm{b}}$	RSRP of UE i in ABS period and normal period
RSRP_i'	RSRP of UE i from neighbor eNB
$R_i^{\mathrm{M,a}}$,$R_i^{\mathrm{P,b}}$	Rate of marco and pico user in ABS and normal period

In this work, we consider MUEs are associated to the M-ENB and PUEs are associated to the P-ENBs without going into the details of user association, because the research of user association has gained considerable attention in the past. In macro-cell, user association is always based on maximum reference signal received power (RSRP). However, in the HetNets, the pico-cells always use the Pico/Femto eNBs, which have lower transmission power and smaller coverage. Therefore, traditional Max-RSRP based on user association might lead to unbalanced load between the pico-cell and the macro-cell. The network-wide user association problem for HetNets is NP-hard in general [12]. In order to solve the load balance problem, cell range expansion [13] has been proposed by setting a cell associated biasing within RSRP when UEs try to connect to P-eNBs. By this way, UEs can connect the P-eNB, although this P-eNB might not be given the best RSRP at the user side, compared with M-eNB. Cell range expansion is always deployed in the eICIC algorithm to balance network load. The influence of cell range expansion was discussed in the load balance scheme presented in [12]. In our research, the cell range expansion also has impact when we combine the eICIC and CoMP. The details will be discussed in Section 4.

As mentioned above, all PUEs share the same spectrum with M-eNB and dense distribution, then M-eNB might cause high inter-cell interference to the PUEs which associate with P-eNB in cell range expansion area. And due to the close distance between each pico-cell, the intra-cell interference is also considerable. That is why we set the inter-cell and intra-cell interference cancellation as our main objective. A hybrid interference management based on dynamic ABS and CoMP is proposed in this paper to eliminate these two types of interference.

Before proceeding to problem formulation, we give the notations first and that will be used in the rest of the paper, as shown in Table 1.

3 Hybrid interference management algorithm

3.1 Virtual cell building

Figure 2 shows more than 20 pico-cells in one macro-cell, and at least 6 pico-cells in one sector in the network. It is too complicated to manage every pico-cell separately, and this will cause a serious problem of signaling overhead while deploying interference management scheme. Therefore, the concept of virtual cell is used to simplify the network structure. A virtual cell consists of pico-cells based on their geographic locations and channel conditions. Unlike femto-eNB, pico-eNB is always deployed by operators in a fixed position, such as the signal blind zone or overload zone in macro-cells. Under these conditions, the location of pico-eNBs is logical but uneven. We use a fast algorithm to select members of virtual cell.

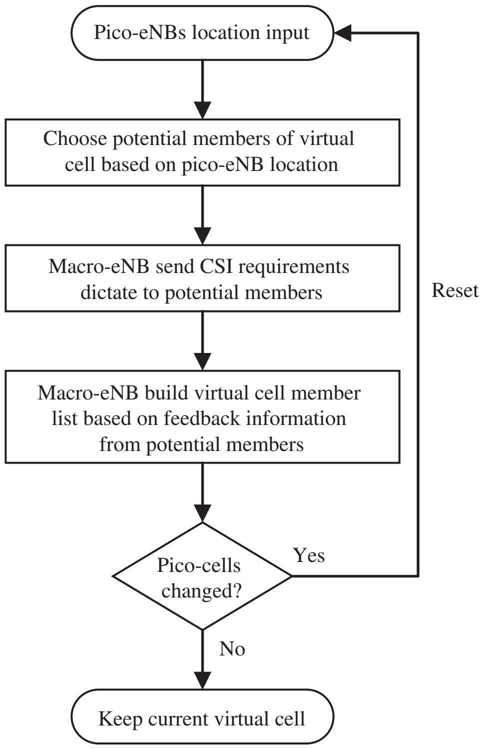

Figure 3 Flow chart of virtual cell building.

Firstly, the network can get the location information of the pico-eNBs in macro-cell, then pico-eNBs, which are located close to each other, will be chosen as potential members in the list. Secondly, the Macro-eNB sends channel state information (CSI) requirements to these potential members through X2 interface [14], and these pico-cells return the average CSI of its own UEs. Based on the CSI information, the pico-cells which all have the poor channel quality will be chosen as the virtual cell members. Because these pico-cells are close to each other and have similar channel quality, which means they are 'sharing' similar interference, this virtual cell can be deployed for interference management effectively. In some situation, the pico-eNBs might be deactivated or migrate by operator, which will change the channel environment, although it is not frequently happened. In this context, the scheme of virtual cell is set semi-static, which will reset when the changes of pico-eNBs are detected. The flow chart is given in Figure 3.

3.2 Joint dynamic eICIC scheme

In order to improve the frequency efficiency, the M-eNB and the virtual cell share the same frequency. If a PUE uses the same physical resource block (PRB) as that used by the M-eNB, this PUE will experience interferences from M-eNB, and vice versa. This type of interference might be insignificant if the PUE is in the center of virtual cell and sees a weak signal from M-eNB. However, if the PUE moves to the edge of virtual cell, the M-eNB to PUE interference will be considerable.

To eliminate the inter-interference, the effective solution is to allocate different and orthogonal PRBs to MUE and PUE. As mentioned above, M-eNB and P-eNB share the same spectrum, then a dynamic eICIC algorithm is deployed in network. The main target is to improve overall throughput by eliminating the inter-cell interference, as shown in (1). M-eNB transmits ABS time-division multiplexed with normally transmitted subframes according to a dynamic ABS pattern of a specified duration. We try to dynamically change the fraction of ABS, and the throughput of macro-cells and virtual-cells can be expressed as follows:

$$\max_{\alpha} R^{\mathrm{M}} + R^{\mathrm{V}}, \tag{1}$$

$$R^{\mathrm{M}} = \eta_b \eta_c \sum_{i=1}^{M} \left[\alpha \log_2 \left(1 + \frac{\mathrm{RSRP}_i^{\mathrm{M,a}}}{\left(\mathrm{RSRP}_i' + \delta^2\right)\eta_s} \right) + (1-\alpha) \log_2 \left(1 + \frac{\mathrm{RSRP}_i^{\mathrm{M,b}}}{\left(\mathrm{RSRP}_i' + \delta^2\right)\eta_s} \right) \right], \tag{2}$$

$$R^{\mathrm{V}} = \eta_b \eta_c \sum_{i=1}^{N \cdot L} \left[\alpha \log_2 \left(1 + \frac{\mathrm{RSRP}_i^{\mathrm{P,a}}}{\delta^2 \eta_s} \right) + (1-\alpha) \log_2 \left(1 + \frac{\mathrm{RSRP}_i^{\mathrm{P,b}}}{\left(\mathrm{RSRP}_i' + \delta^2\right)\eta_s} \right) \right]. \tag{3}$$

Three parameters η_b, η_c and η_s, in (2) and (3), are used to model the throughput of practical LTE systems [15]. The first parameter represents the system bandwidth efficiency and accounts for different overheads such as cyclic-prefixes and pilots. The other two parameters are jointly used to model SINR implementation efficiency to match receiver algorithms and its supported modulation-coding schemes (MCS) [15]. Using a practical formula for throughput in network rather than the Shannon capacity formula can provide closer approximation to real implementations and improve the algorithm accuracy appreciably.

From (2) and (3), it is obvious that virtual cell channel performance can be improved while ABSs increase, at the cost of the decrease of MUEs throughput. The CoMP technology is deployed in the network, and its key point is multi-user beamforming [16]. Based on multiple-output (MIMO) channels, phase-shift is added to the data vector with obvious peak reduction. In order to focus on interference management, we consider effects of multi-user beamforming without details. Due to the deployment of multi-user beamforming in macro-cell, PUE and MUE will not interfere with each other if they are far from each other while using the same PRB. From [17], the horizontal and vertical antenna patterns in beamforming can be expressed as

$$A_H(\varphi) = -\min \left[12 \left(\frac{\varphi}{\varphi_{3\mathrm{dB}}} \right)^2, A_m \right], \tag{4}$$

$$A_H(\Theta) = -\min \left[12 \left(\frac{\Theta - \Theta_{\mathrm{etilit}}}{\Theta_{3\mathrm{dB}}} \right)^2, \mathrm{SLA}_v \right]. \tag{5}$$

The parameter Θ_{etilit} is the electrical antenna downtilt. The value of this parameter and a potential additional mechanical tilt is not given here but may be set according to other RRM techniques used. For calibration purposes, the values $\Theta_{\mathrm{etilit}} = 15^\circ$ for 3GPP case 1 and $\Theta_{\mathrm{etilit}} = 6^\circ$ for 3GPP case 3. The antenna height at the base station is 32 m, and the antenna height at UE is 1.5 m. The method for combining the 3D antenna patterns can be expressed as

$$A_H(\Theta, \varphi) = -\min \left\{ -[A_H(\varphi) + A_V(\Theta)], A_m \right\}. \tag{6}$$

The antenna gain is considered in the RSRP of every user. In this case, we can further increase the spectrum efficiency by splitting the ABS in frequency domain In other words, different PRBs will implement different ABS models. In this way, MUEs can keep the transmission in some ABSs which are supposed to remain silent for them, as long as the interference is not considerable, as illustrated in Figure 2. A novel ABS strategy we proposed can significantly increase the spectrum efficiency of macro-cell in the eICIC scheme, and virtual cell channel performance can be improved without obvious decrease of MUEs throughput.

In this case, the fraction of ABS should change both in time domain and frequency domain, so as to get adapted to network dynamics. Therefore, we consider the throughput of every PRB instead of the rate of every UE. The target of our scheme is to maximize the throughput of whole PRBs while meeting QoS constrains for MUEs and PUEs. And the rate of MUE in the downlink is discussed as follows:

$$R^{\mathrm{M}} = \eta_b \eta_c \sum_{i=1}^{\mathrm{PRB}^{\mathrm{M}}} \left[\alpha_i R^{\mathrm{M,a}} + (1-\alpha_i) R^{\mathrm{M,b}} \right], \tag{7}$$

where $\mathrm{PRB}^{\mathrm{M}}$ represents the PRB used by MUE, and α_i is the ABS faction deployed on current PRB_i. The throughput of MUEs should comprise two parts, the throughput in ABS period and the throughput in nomal period, for each PRB. If this PRB is used by MUE and PUE during ABS period and the interference is intolerant, the transmission of MUE should be suspended. Consequently, $\mathrm{RSRP}_i^{\mathrm{M,a}}$ in (2) should be naught. But if the interference is negligible, MUE is allowed to keep the transmission, in other words, ABS is not necessary. Constraint (8) imposes a lower limit R_{T} on the throughput of MUE, which represents the QoS requirement. This parameter R_{T} is pre-determined which can be changed by network operators to meet different needs.

$$R_i^{\mathrm{M}} > R_{\mathrm{T}}, \quad i \in \mathrm{MUE}. \tag{8}$$

On the other hand, the throughput of PUE in the downlink also comprises two parts, the throughput in ABS period and the throughput in nomal period, for each PRB, which can be expressed similarly as follows:

$$R^{\mathrm{V}} = \eta_b \eta_c \sum_{i=1}^{\mathrm{PRB}^{\mathrm{P}}} [\alpha_i R^{\mathrm{P,a}} + (1-\alpha_i) R^{\mathrm{P,b}}]. \tag{9}$$

The constraint in (10) represents the value space for fraction of ABS. $\alpha_{\max}$ is preset to avoid some rare cases, for example, all frame is full of ABS, and as a result, MUE cannot transmit any data in the current network. For our simulation, $\alpha_{\max}$ is preset to 6/8 normally. And constraint (11) represents that change of network rate must be positive after ABS ratio is changed.

$$0 < \alpha_i < \alpha_{\max}, \quad i \in \mathrm{PRB}, \tag{10}$$

$$\Delta R_i^{\mathrm{M}} + \Delta R_i^{\mathrm{P}} > 0, \quad i \in \mathrm{PRB}. \tag{11}$$

The optimal model is then to maximize the sum rate of overall PRB rate while meeting the constraints. The predetermined cell association bias can be fixed or updated semi-statically from feedback. The constraints can be formulated as follows:

$$\max_{\alpha_i} \sum_{i}^{\mathrm{PRB}} (R_i^{\mathrm{M}} + R_i^{\mathrm{P}}) \tag{12}$$

$$\text{s.t.} \quad (8), (10), (11). \tag{13}$$

3.3 Virtual cell based joint transmission scheme

Intra-cell interference is another obstacle to network performance improvement except for inter-cell interference. With the development of ultra-dense HetNet, intra-cell interference is getting worse while distance shrinks between pico-cells. Our simulation finds a special phenomenon: after the inter-cell interference management is deployed, the signal strength is significantly increased, however, the interference between pico-cells is also getting worse at the same time. This means that the inter-cell interference management is a double-edged sword to virtual cells, and the effective intra-cell interference management is an indispensable part.

To solve this problem, the downlink joint transmission scheme is applied to eliminate the intra-interference among virtual cells. The characteristics of virtual cell are introduced in Subsection 3.1, which can be summarized as follows: (1) short distance between pico-cells; (2) similar channel states. Apparently, the virtual cell fits well with joint transmission in CoMP. Due to the close range between the P-eNBs, some PUEs might receive strong signals from more than one P-eNB, especially for the cell-edge user. Then, this kind of PUEs can be chosen as coordinated users which can connect coordinate eNBs simultaneously and the Pico-eNBs which provide strong signals can be chosen as coordinate eNBs. Like multi-user beamforming, we concentrate on effects of joint transmission in interference management without details in physical layer. Theoretically, every member in virtual cell is a potential coordinate eNB, but in the real network, some pico-eNBs in virtual cell might be overloaded or cannot provide good signal to anyone. These pico-eNBs are not suitable for coordinate transmission, and only the pico-eNBs which interfere with others will be chosen as coordinate eNBs.

As for the selection of coordinated UEs, it will be easy to find out that any PUE suffering from neighbor Pico-eNBs can be chosen as the coordinated UEs. These PUEs will upload RSRP list, and the eNB which has the best RSRP will be its coordinate eNB, except for the original base station. The constraint of coordinated association can be expressed as (14). Constraint (14) represents that PUEs can be chosen as coordinated users only if the RSRP from coordinate BS reaches or exceeds the threshold $\mathrm{RSRP_T}$, which is preset by network operators.

$$\mathrm{RSRP_{CSB}} > \mathrm{RSRP_T}. \tag{14}$$

In the joint transmission, the strong signal from neighbor eNB can be used as transmission signal instead of interference, which means the original interference power should be counted as receive power. Hence, the rate of virtual cell in (9) can be rewritten as (15).

$$R^{\mathrm{V}} = \eta_b \eta_c \sum_{i=1}^{\mathrm{PRB^P}} \left[\alpha \log_2 \left(1 + \frac{\sum_j^{\mathrm{CSB}} \mathrm{RSRP}_{i,j}^{\mathrm{P,a}}}{\delta^2 \eta_s} \right) + (1-\alpha) \log_2 \left(1 + \frac{\sum_j^{\mathrm{CSB}} \mathrm{RSRP}_{i,j}^{\mathrm{P,b}}}{\left(\mathrm{RSRP}_i' + \delta^2\right) \eta_s} \right) \right]. \tag{15}$$

If the signal from neighbor P-eNB is not strong enough, in other words, the interference is not severe, then the PUE will keep current connection with original P-ENB. In this case, the intra-cell interference can be effectively inhibited, nonetheless, we cannot consider the virtual cell and macro-cell separately. If an MUE moves around the edge area of the virtual cell, it will suffer interference from the virtual cell, although it is not common. And sometimes, some MUEs are moving in the virtual cell but still cannot access the pico-eNB due to closed subscriber group (CSG) [18]. Therefor the constraint of interference between virtual cell and MUE is necessary. In this case, power allocation has attracted wide attention in CoMP [19–21], which can eliminate the interference greatly. In order to prevent the interference between MUE and virtual cell, constraint (16) is built to limit the P-eNB transmit power. If an MUE is moving around the virtual cell and experiencing strong interference from the virtual cell, it will send high interference indicator (HII) to the macro-cell, then P-ENB will receive the indicator to reduce the power through the X2 interface. The threshold I_{T} is also preset by the network operator, like the $\mathrm{RSRP_T}$.

$$I_i^{\mathrm{M}} < I_{\mathrm{T}}. \tag{16}$$

Taken together, the overall optimization model is given as follows:

$$\max_{\alpha_i, p_i} \sum_i^{\mathrm{PRB}} (R_i^{\mathrm{M}} + R_i^{\mathrm{P}}) \tag{17}$$

$$\text{s.t.} \quad (8), (10), (11), (14), (16). \tag{18}$$

4 Solution of the optimization problem

The optimization factor PRB is resource block both in time-domain and frequency domain. Hence, the rate and the power in one frame with different PRBs can be formulated as a $1 \times F$ vector, which can be rewritten as

$$\boldsymbol{R} = [R_1, R_2, \ldots, R_{\mathrm{F}}]^{\mathrm{T}}, \tag{19}$$

$$\mathbf{P} = [P_1, P_2, \ldots, P_{\mathrm{F}}]^{\mathrm{T}}. \tag{20}$$

ABS ratio α in different PRBs can also be formulated as a vector, considering it is a parameter in time-domain only, which can be rewritten as

$$\boldsymbol{\alpha} = [\alpha_1, \alpha_2, \ldots, \alpha_{\mathrm{F}}]. \tag{21}$$

The optimization problem can be rewritten as

$$\max_{\boldsymbol{\alpha}, \boldsymbol{P}} \boldsymbol{\alpha} \times \boldsymbol{R}^{\mathrm{ABS}} + \boldsymbol{\beta} \times \boldsymbol{R}^{\mathrm{non-ABS}} \tag{22}$$

$$\text{s.t.} \quad (8), (10), (11), (14), (16). \tag{23}$$

In (22), vector $\boldsymbol{\beta}$ represents the vector consisting of $1-\alpha_i$, which can be formulated as $\boldsymbol{\beta} = [1-\alpha_1, 1-\alpha_2, \ldots, 1-\alpha_{\mathrm{F}}]$. Vector $\boldsymbol{R}^{\mathrm{ABS}}$ and $\boldsymbol{R}^{\mathrm{non-ABS}}$ represent the throughput in ABS period and non-ABS period in each PRB. And the constraints (8), (10), (11), (14), (16) are also adjusted to fit the vector. To simplify the model, (22) can be rewritten as

$$\max_{\boldsymbol{\alpha},\boldsymbol{P}} \boldsymbol{\alpha} \times (\boldsymbol{R}^{\mathrm{ABS}} - \boldsymbol{R}^{\mathrm{non-ABS}}) + \boldsymbol{A} \times \boldsymbol{R}^{\mathrm{non-ABS}}. \tag{24}$$

We define F dimensional unit vector $\boldsymbol{A} = [1, \ldots, 1]_{\mathrm{F}}$ to make sure that the computation is a number. Due to the independence of two stages of interference management, $\boldsymbol{\alpha}$,$\boldsymbol{P}$ are also independent of each other, so we can solve the optimization problem respectively. For optimal ABS ratio, obviously, (24) is a linear function which is continuous in [0, 1], and, it is a monotone function inside the domain where maximum should converge to the function boundaries. Then, the optimal ABS ratio $\boldsymbol{\alpha}^*$ can be expressed as

$$\boldsymbol{\alpha}^* = \begin{cases} \boldsymbol{\alpha}_{\max}, & \boldsymbol{R}^{\mathrm{ABS}} \geqslant \boldsymbol{R}^{\mathrm{non-ABS}}, \\ 0, & \boldsymbol{R}^{\mathrm{ABS}} < \boldsymbol{R}^{\mathrm{non-ABS}}, \end{cases} \tag{25}$$

which can also be represented as

$$\boldsymbol{\alpha}^* = \boldsymbol{\alpha}_{\max} \cdot \mathscr{U}(\boldsymbol{R}^{\mathrm{ABS}} - \boldsymbol{R}^{\mathrm{non-ABS}}). \tag{26}$$

The $\mathscr{U}(\cdot)$ in (26) is the step function and $\boldsymbol{\alpha}_{\max}$ represents the maximum in domain of values. After $\boldsymbol{\alpha}^*$ is solved, $\boldsymbol{P}^*$ can be found by a power control algorithm, as shown in Algorithm 1. We set a T_{I} timer to ensure that the interference appears frequently, rather than by accident.

Algorithm 1 Power control algorithm

Require: $\mathrm{RSRP}_{\mathrm{P}}^{\mathrm{M}}, I_{\mathrm{T}}$;
Ensure: P^*;
while $\mathrm{RSRP}_{\mathrm{P}}^{\mathrm{M}} > 0$ **do**
  Collect the Pico-eNB ID from $\mathrm{RSRP}_{\mathrm{P}}^{\mathrm{M}}$ information;
  if $\mathrm{RSRP}_{\mathrm{P}}^{\mathrm{M}} > I_{\mathrm{T}}$ **then**
    Start the T_{I} timer;
    if T_{I} timer countdown to the end$||\mathrm{RSRP}_{\mathrm{P}}^{\mathrm{M}} > I_{\mathrm{T}}$ **then**
      Macro-eNB send HII to the pico-eNB;
      while $\mathrm{RSRP}_{\mathrm{P}}^{\mathrm{M}} < I_{\mathrm{T}}$ **do**
        The pico-eNB reduce transmit power $P_{\mathrm{p-eNB}}$;
      end while
    else if $\mathrm{RSRP}_{\mathrm{P}}^{\mathrm{M}} < I_{\mathrm{T}}$ **then**
      Reset T_{I} timer;
    end if
  end if
  $P^* = P_{\mathrm{p-eNB}}$
end while

5 Performance evaluation

In this section, we evaluate the performance of the hybrid interference management against various baseline schemes.

5.1 Simulation setup

We build a Matlab system level simulation platform based on Matlab according to 3GPP standardization [17]. In order to go on with a simulation with high efficiency, we simplify the specific process of protocol stack to focus on the changes of network load, and the proportional fair scheduling algorithm to ensure the fairness in system while users are distributed randomly in cell coverage. Schemes under

Table 2 Simulation parameters

Layout	Parameters
Bandwidth (M-eNB, P-eNB)	10 MHz, 10 MHz
M-ENB transmit power	43 dBm
P-ENB transmit power	30 dBm
Cell radius (M-eNB, P-eNB)	500 m, 50 m
Noise figure	148.95 dB
Macro path loss model	128.1+37.6log10(R) (R[km])
Pico path loss model	140.7+36.7log10(R) (R[km])
Number of PRBs	50
Subframe duration	1 ms
Traffic model	Full-buffer
Cell association bias	8 dB
η_b, η_c and η_s	0.42, 1, 0.62

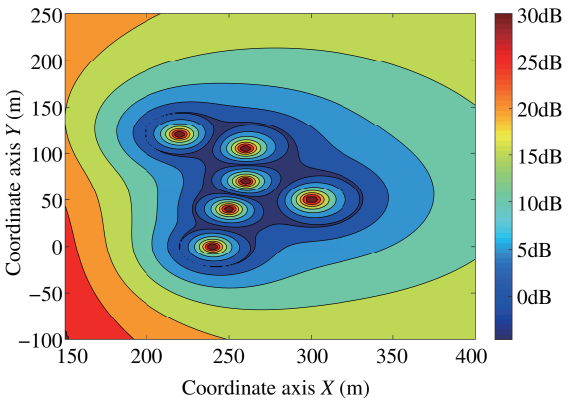

Figure 4 Distribution of virtual cell SINR without scheme.

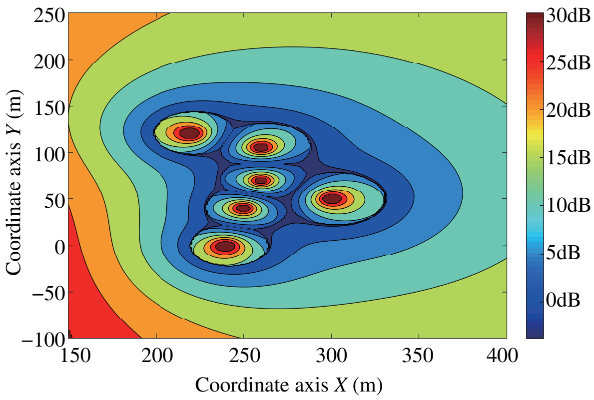

Figure 5 Distribution of virtual cell SINR with eICIC scheme.

comparison use the same deployment scenario in Figure 1 consisting of one M-ENB, six P-ENBs in one section, M MUEs, S PUEs in the cell center and at the cell edge. As we mentioned above, M-ENB and P-ENBs will share the same frequency to improve the spectrum efficiency, and we use the simulation parameters summarized in Table 2. η_b represents the system bandwidth efficiency and accounts for different overheads such as cyclic-prefixes and pilots, and η_c, η_s are jointly used to model SINR implementation efficiency due to receiver algorithms and its supported modulation-coding schemes (MCS). These three parameters are used to model the throughput of practical LTE system. For our simulations, we use $\eta_b = 0.42$, $\eta_c = 1$, and $\eta_s = 0.62$.

5.2 Results

We compare different schemes for performance evaluation. These schemes use the same system layout in Table 2 with different interference management.

Firstly, SINRs in virtual cells are compared in circumstances of no interference, eICIC-only deployment, and hybrid interference management respectively. As shown in Figure 4, the color gradation is lighter in the center of virtual cell compared with Figure 5, which means the SINR is improved after eICIC is deployed in the network. However, intra-cell interference around pico-cell edge is increasing with the increase of signal strength of every P-eNB. As a result, pico-cells are extruded and compressed by each other as shown in Figure 5. This provides a good condition to deploy CoMP at the same time. Figure 6 shows that SINR can be significantly improved by CoMP at the cell edge, which also leads to the increase

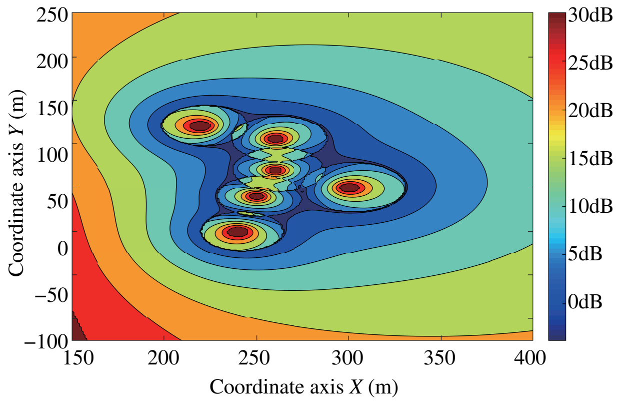

Figure 6 Distribution of virtual cell SINR with proposed scheme.

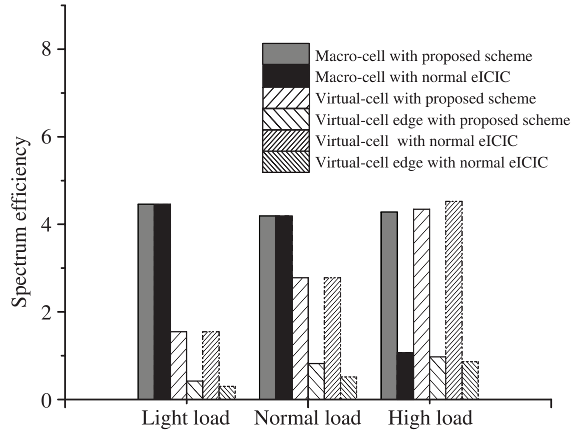

Figure 7 Comparison of spectrum efficiency with different schemes.

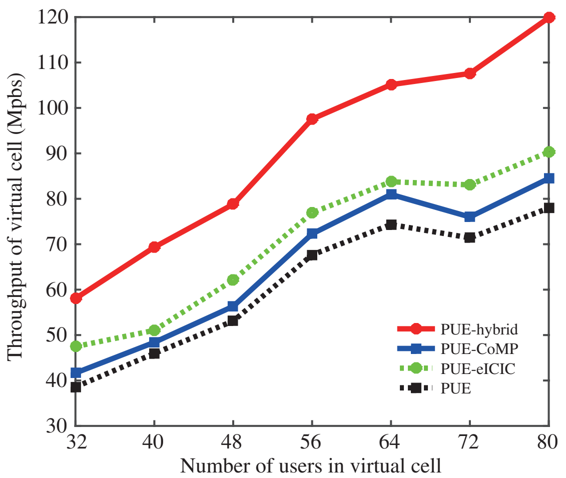

Figure 8 Throughput of virtual cell in different schemes.

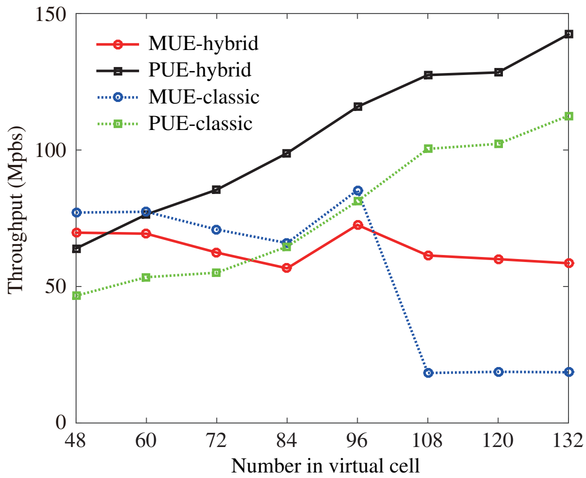

Figure 9 Throughput of MUE in different schemes.

of spectrum efficiency.

Figure 7 shows the comparison of the spectrum efficiency between different schemes. As for the spectrum efficiency of macro cell, there are no differences between the normal eICIC scheme and the proposed scheme when network load is light. However, the spectrum efficiency decreases sharply with the increase of network load for normal eICIC scheme. This is because ABS ratio is increased when virtual cell load is improved. Higher ABS ratio leads to less resources for MUE, which causes the drop of MUE throughput. Due to multi-user beamforming, the proposed scheme can keep the average level of spectrum efficiency, but in some simulations the spectrum efficiency also decreases slightly. And the spectrum efficiency of virtual cell edge is improved by the joint transmission, while the average level is close to each other.

The classic solution of interference management is compared with the proposed scheme in Figures 8 and 9. Users are distributed randomly, which causes the curves to fluctuate. In Figure 8, the CoMP scheme and the eICIC scheme are adopted respectively. The throughput of virtual cell may benefit from both of the two schemes, and the gain of eICIC scheme is greater than the other one. This is because the signal from neighbor P-ENB is not strong enough while considering the inter-interference from M-ENBs with the deployment of CoMP scheme. As seen in Figure 8, hybrid interference management can achieve the best performance, which is more than the sum of two gains. Due to the good channel condition in ABS, SINR in virtual cell can be increased obviously, and as a result, the signal strength from coordinate P-ENBs is significantly enhanced, which leads to a better performance in CoMP scheme. As shown in

Figure 9, the increase of throughput from virtual cell is higher than others when the proposed scheme is deployed, and the throughput of MUE is not decreased heavily (red curve) compared with traditional eICIC scheme (blue curve). This is because in the traditional eICIC scheme, deploying ABS can reduce the transmission time for MUE However, in the proposed scheme due to the multi-user beamforming, only MUE close to virtual cellS needs to remain silent. In the hybrid scheme MUE can keep the transmission. Therefore, in a classical interference management scheme, MUEs will have few subframes to transmit data when virtual cells have a higher load. As a result, the throughput of MUEs decreases sharply.

All in one, the proposed scheme can produce "a whole greater than the sum of the parts ". This means the hybrid interference management scheme is not just a simple combination of two interference schemes, but an effective interference management scheme suitable for the ultra-dense pico-cell in HetNets, which can avoid rapid decrease of spectrum efficiency.

6 Conclusion

This paper focuses on the optimization of throughput in ultra-dense HetNets with the hybrid interference management strategy. Simulation results show that the proposed scheme has better dynamic performance while compared with the traditional interference management. It avoids the sharp decrease of spectrum efficiency in ultra-dense HetNets. With the consideration of dynamic cell range extension, we will find some new strategies such as by choosing coordinate base stations.

Acknowledgements This work was supported by National Natural Science Foundation of China (Grant Nos. 61571073, 61171111), National High-Tech R&D Program of China (863) (Grant No. 2014AA01A701), National Science and Technology Major Project (Grant No. 2014ZX03003010-004), and Innovation Project Foundation for postgraduate student of Chongqing (Grant No. CYS14141).

Conflict of interest The authors declare that they have no conflict of interest.

References

1 Deb S, Monogioudis P, Miernik J, et al. Algorithms for enhanced inter-cell interference coordination (eICIC) in LTE HetNets. ACM Trans Netw, 2014, 22: 137–150
2 Vasudevan S, Pupala R N, Sivanesan K. Dynamic eICICA proactive strategy for improving spectral efficiencies of heterogeneous LTE cellular networks by leveraging user mobility and traffic dynamics. IEEE Trans Wirel Commun, 2013, 12: 4956–4969
3 Liu A, Lau V K N, Ruan L, et al. Hierarchical radio resource optimization for heterogeneous networks with enhanced inter-cell interference coordination (eICIC). IEEE Trans Signal Process, 2014, 62: 1684–1693
4 Zhang Y P, Feng S, Zhang P. Adaptive cell association and interference management in LTE-A small-cell networks. In: Proceedings of Vehicular Technology Conference (VTC Fall), Las Vegas, 2013. 1–6
5 Zhang Y P, Feng S L, Zhang P, et al. Inter-cell interference management in LTE-A small-cell networks. In: Proceedings of Vehicular Technology Conference (VTC Fall), Dresden, 2013. 1–6
6 Peng M, Li Y, Zhao Z, et al. System architecture and key technologies for 5G heterogeneous cloud radio access networks. IEEE Netw, 2015, 29: 6–14
7 Li M, Collings I B, Hanly S V, et al. Multicell coordinated scheduling with multiuser zero-forcing beamforming. IEEE Trans Wirel Commun, 2015, 15: 827–842
8 Li Y N R, Li J, Li W, et al. CoMP and interference coordination in heterogeneous network for LTE-advanced. In: Proceedings of Globecom Workshops, Shenzhen, 2012. 1107–1111
9 Visotsky E, Mondal B, Thomas T, et al. Joint scheduling for CoMP and eICIC in heterogeneous network deployments. In: Proceedings of Vehicular Technology Conference (VTC Spring), Arlington Heights, 2013. 1–5
10 Du H T, Zhou W A, Lu X Q, et al. An optimized resource allocation and CoMP based interference coordination scheme for LTE-A Het-Net. In: Proceedings of 9th International Conference on Broadband and Wireless Computing, Communication and Applications (BWCCA), 2014, Guangdong. 207–211
11 Kim J, Lee H W, Chong S. Virtual cell beamforming in cooperative networks. IEEE J Sel Areas Commun, 2014, 32: 1126–1138
12 Ye Q Y, Rong B Y, Chen Y D, et al. User association for load balancing in heterogeneous cellular networks. IEEE Trans Wirel Commun, 2013, 12: 2706–2716
13 Miyashita M, Mikami M, Fujii T. Investigation on inter-cell interference cancellation scheme for small-cell user equipments in heterogeneous networks employing cell range expansion. In: Proceedings of Vehicular Technology Conference

(VTC Spring), Tokyo, 2015. 1–5
14 3GPP TS 36.423 V13.1.0, X2 application protocol (Release 13), 2015
15 Mogensen P, Wei N, Kovacs I, et al. LTE capacity compared to the Shannon bound. In: Proceedings of Vehicular Technology Conference, Dublin, 2007. 1234–1238
16 Rim M. Multi-user downlink beamforming with multiple transmit and receive antennas. Electron Lett, 2002, 38: 1725–1726
17 Evolved Universal Terrestrial Radio Access (E-UTRA), Further advancements for E-UTRA physical layer aspects (Release 9), 3rd Generation Partnership Project. Sophia-Antipolis Cedex, France, 2010: 3GPP TS 36.814, v9.0.0
18 Lembo S, Lunden P, Tirkkonen O, et al. Optimal muting ratio for Enhanced Inter-Cell Interference Coordination (eICIC) in HetNets. In: Proceedings of Communications Workshops (ICC), Aalto, 2013. 1145–1149
19 Fu S, Wu B, Wen H, et al. Transmission scheduling and game theoretical power allocation for interference coordination in CoMP. IEEE Trans Wirel Commun, 2014, 13: 112–123
20 Hunukumbure M, Vadgama S. Improving cell edge energy efficiency through CoMP beam-forming. In: Proceedings of Vehicular Technology Conference (VTC Spring), Hayes, 2013. 1–5
21 Qiang L, Yang Y, Shu F, et al. Coordinated beamforming in downlink CoMP transmission system. In: Proceedings of 5th International ICST Conference on Communications and Networking in China (CHINACOM), Beijing, 2010. 1–5